

## THE SELF-SIMILARITY OF THE CIRCUMGALACTIC MEDIUM WITH GALAXY VIRIAL MASS: IMPLICATIONS FOR COLD-MODE ACCRETION

CHRISTOPHER W. CHURCHILL<sup>1</sup>, NIKOLE M. NIELSEN<sup>1</sup>, GLENN G. KACPRZAK<sup>2,3</sup>, AND SEBASTIAN TRUJILLO-GOMEZ<sup>1</sup>

*Submitted to ApJL, November 2, 2012*

### ABSTRACT

We apply halo abundance matching to obtain galaxy virial masses,  $M_h$ , and radii,  $R_{\text{vir}}$ , for 183 “isolated” galaxies from the “Mg II Absorber-Galaxy Catalog” (MAGII-CAT). All galaxies have spectroscopic redshifts ( $0.07 \leq z \leq 1.12$ ) and their circumgalactic medium (CGM) is probed in Mg II absorption within projected galactocentric distances  $D \leq 200$  kpc. We examine the behavior of equivalent width,  $W_r(2796)$ , and covering fraction,  $f_c$ , as a function of  $D$ ,  $D/R_{\text{vir}}$ , and  $M_h$ . Bifurcating the sample at the median mass  $\log M_h/M_\odot = 12$ , we find: [1] systematic segregation of  $M_h$  on the  $W_r(2796)$ – $D$  plane ( $4.0 \sigma$ ); high-mass halos are found at higher  $D$  with larger  $W_r(2796)$  compared to low-mass halos. On the  $W_r(2796)$ – $D/R_{\text{vir}}$  plane, mass segregation vanishes and we find  $W_r(2796) \propto (D/R_{\text{vir}})^{-2}$  ( $8.9 \sigma$ ); [2] high-mass halos have larger  $f_c$  at a given  $D$ , whereas  $f_c$  is independent of  $M_h$  at all  $D/R_{\text{vir}}$ ; [3]  $f_c$  is constant with  $M_h$  over the range  $10.7 \leq \log M_h/M_\odot \leq 13.9$  within a given  $D$  or  $D/R_{\text{vir}}$ . The combined results suggest the Mg II absorbing CGM is self-similar with halo mass, even above  $\log M_h/M_\odot \simeq 12$ , where cold mode accretion is predicted to be quenched. If theory is correct, either outflows or sub-halos must contribute to absorption in high-mass halos such that low- and high-mass halos are observationally indistinguishable using Mg II absorption strength once impact parameter is scaled by halo mass. Alternatively, the data may indicate predictions of a universal shut down of cold-mode accretion in high-mass halos may require revision.

*Subject headings:* galaxies: halos — quasars: absorption lines

### 1. INTRODUCTION

Direct observation of the circumgalactic medium (CGM) is important for exposing the link between the intergalactic medium and galaxies, and the processes governing their star formation histories, stellar masses, luminosities, and morphologies. The CGM harbors a reservoir of chemically enriched gas with a mass that may rival the gas reservoir in galaxies (Tumlinson et al. 2011). The Mg II  $\lambda\lambda 2796, 2803$  absorption doublet observed in quasar spectra is an ideal probe of the CGM (see Churchill, Kacprzak, & Steidel 2005, for a review); it traces low-ionization gas over the broad range  $10^{16.5} \leq N(\text{H I}) \leq 10^{21.5} \text{ cm}^{-2}$  (Churchill et al. 1999, 2000; Rao & Turnshek 2000; Rigby, Charlton, & Churchill 2002) and is detected out to projected distances of  $\sim 150$  proper kpc (Kacprzak et al. 2008; Chen et al. 2010a; Churchill et al. 2012a; Nielsen, Churchill, & Kacprzak 2012).

In general, the CGM is a complex dynamical region affected by accretion, winds, and mergers. Two distinct modes of accretion are theorized to operate, “hot” or “cold”, where the mode depends on whether the halo mass,  $M_h$ , is above or below a critical threshold  $M_{\text{crit}}$ , where  $\log M_{\text{crit}}/M_\odot \sim 12$  (e.g., Birnboim & Dekel 2003; Kereš et al. 2005; Dekel & Birnboim 2006; Kereš et al. 2009; Stewart et al. 2011; van de Voort et al. 2011). Cold-mode accretion is predicted in  $M_h < M_{\text{crit}}$  halos, whereas hot-mode is predicted in  $M_h > M_{\text{crit}}$  halos. Though some observations provide plausible evidence for cold-mode accretion at  $z < 1$  (Kacprzak et al. 2011; Ribaudo et al. 2011; Thom et al. 2011; Kacprzak et al. 2012), the baryonic mass in the cold mode is expected to diminish with decreasing redshift.

If accretion dominates, the distribution of absorber equiv-

alent widths,  $W_r(2796)$ , and the absorption covering fraction,  $f_c$ , are predicted to markedly decline in  $M_h > M_{\text{crit}}$  halos. If a large reservoir of cold gas ( $T \sim 10^4$ – $10^5$  K) is present in the CGM of  $M_h > M_{\text{crit}}$  halos, it could imply outflows (cf., Stewart et al. 2011). Indeed, winds are commonly observed in Mg II absorption (e.g., Tremonti et al. 2007; Martin & Bouché 2009; Weiner et al. 2009; Rubin et al. 2010; Martin et al. 2012). Alternatively, the increased number of sub-halos associated with higher mass halos (Klypin et al. 2011) could counteract the predicted behavior of  $W_r(2796)$  and  $f_c$ .

To observationally examine the validity of the hot/cold accretion theoretical paradigm, we require the halo masses of galaxies associated with absorption systems. A robust method for determining these masses is the parameterless halo abundance matching technique (e.g., Conroy et al. 2006; Conroy & Wechsler 2009; Behroozi, Conroy, & Wechsler 2010; Trujillo-Gomez et al. 2011; Rodriguez-Puebla et al. 2012). The method has been extremely successful at reproducing the two-point correlation function with redshift, luminosity, and stellar mass (Conroy et al. 2006; Trujillo-Gomez et al. 2011), the galaxy velocity function, and the luminosity-velocity and baryonic Tully-Fisher relations (Trujillo-Gomez et al. 2011).

In this *Letter*, we explore the connection between  $M_h$  and the Mg II absorbing CGM and show that the “cold” CGM is self-similar with halo mass over the mass range  $10.7 \leq \log M_h/M_\odot \leq 13.9$ . For this work, we define halo mass as the galaxy virial mass, including dark matter and baryons. In § 2 we describe our galaxy sample and our method to estimate each galaxy’s halo mass. We present our findings in § 3. In § 4, we summarize and provide concluding remarks. Throughout, we adopt a  $h = 0.70$ ,  $\Omega_M = 0.3$ ,  $\Omega_\Lambda = 0.7$  flat cosmology.

<sup>1</sup> New Mexico State University, Las Cruces, NM 88003

<sup>2</sup> Swinburne University of Technology, Victoria 3122, Australia

<sup>3</sup> Australian Research Council Super Science Fellow

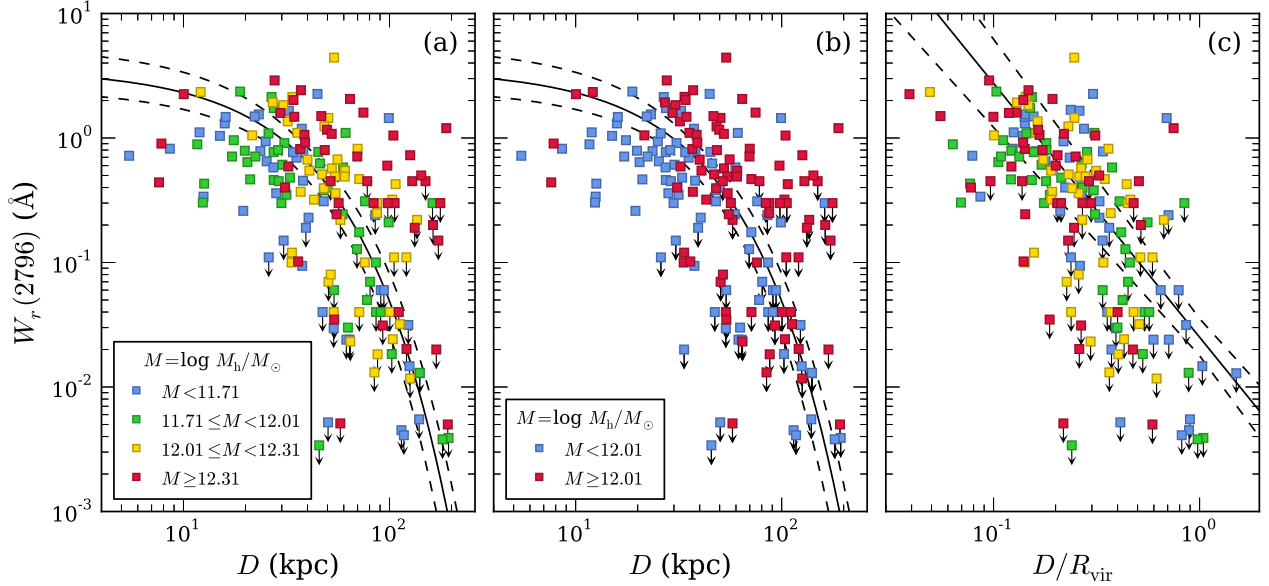


FIG. 1.—  $W_r(2796)$  versus  $D$  and  $D/R_{\text{vir}}$ . Limits are indicated with downward arrows. The solid curve is the fit to the full sample and dashed curves are the  $1\sigma$  envelope. (a) The full sample of galaxies separated into  $M_h$  quartiles. (b) The high-mass and low-mass subsamples. The high- and low-mass subsamples with measured absorption are segregated on this diagram with  $4.0\sigma$  significance. (c)  $W_r(2796)$  versus  $D/R_{\text{vir}}$ , which is anti-correlated with  $8.9\sigma$  significance. The fit yields  $W_r(2796) \propto (D/R_{\text{vir}})^{-2}$ . The mass segregation vanishes.

## 2. THE SAMPLE, VIRAL MASSES, AND VIRIAL RADII

Our sample comprises 183 “isolated” galaxies from the “MgII Absorber-Galaxy Catalog” (MAGII-CAT, Nielsen, Churchill, & Kacprzak 2013). Each galaxy has a spectroscopic redshift ( $0.07 \leq z \leq 1.12$ ). The impact parameter range is  $5.4 \leq D \leq 194$  kpc. The ranges of the AB absolute  $B$ - and  $K$ -band magnitudes are  $-16.1 \geq M_B \geq -23.1$  and  $-16.9 \geq M_K \geq -25.3$ , with rest-frame  $B-K$  colors  $0.04 \leq B-K \leq 4.09$ . Including  $3\sigma$  upper limits, the rest-frame MgII  $\lambda 2796$  equivalent widths have the range  $0.0034 \leq W_r(2796) \leq 2.90$  Å with one system at  $W_r(2796) = 4.42$  Å.

The  $M_h$  for each galaxy was obtained by abundance matching halos in the Bolshoi  $N$ -body cosmological simulation (Klypin et al. 2011) to the observed  $r$ -band luminosity function (LF) from the COMBO-17 survey (Wolf et al. 2003). In short, the method links the luminosity of galaxies to halo properties in a monotonic fashion, reproducing the LF by construction. Following Trujillo-Gomez et al. (2011), we adopt the maximum circular velocity,  $V_c^{\text{max}}$ , and solve for the unique relation  $n(<M_r) = n(<V_c^{\text{max}})$ , which properly accounts for the depth of the potential well and is unambiguously defined for both central halos and sub-halos.

The halos were matched in the five redshift bins centered at  $z = 0.3, 0.5, 0.7, 0.9, 1.1$  of the COMBO-17  $r$ -band LF. The galaxy  $r$ -band absolute magnitudes,  $M_r$ , were determined by  $k$ -correcting (e.g., Kim, Goobar, & Perlmutter 1996) the  $R$ , SDSS  $r$ , or  $HST$ /WFPC F702W observed magnitudes using the actual filter response curves. We employed Coleman et al. (1980) spectral energy distribution (SED) templates from Bolzonella et al. (2000). The adopted SED for each galaxy was obtained by matching its observed color to the redshifted SEDs. The resulting range of  $M_r$  is  $-15.1 \geq M_r \geq -22.7$ .

Scatter between  $M_h$  and  $M_r$  originates from scatter in the  $M_h-V_c^{\text{max}}$  relation due to different formation times of halos with similar mass. After mapping  $M_h$  to  $M_r$ , we account for this scatter by computing the average  $M_h$  in a  $\Delta M_r = 0.1$  bin

centered on the  $M_r$  of the galaxy. Thus, each derived  $M_h$  is interpreted as the average halo mass of a galaxy with  $M_r$ . Varying the bin size  $\Delta M_r$  had virtually no systematic effect nor change in the scatter of each mass estimate.

The primary uncertainty in the derived  $M_h$  is the observed LF. Tests bracketing reasonable extremes of possible systematic errors in the measured LF yield  $M_h$  that are qualitatively unchanged. Full details of our methods and uncertainties are described in Churchill et al. (2013). The masses have the range  $10.74 \leq \log M_h/M_\odot \leq 13.89$  with median  $\log M_h/M_\odot = 12.01$ . Including systematics and scatter, the uncertainties are  $\delta \log M_h \simeq 0.1$  at  $\log M_h/M_\odot = 10$  increasing quasi-linearly to  $\delta \log M_h \simeq 0.35$  at  $\log M_h/M_\odot = 13$ .

We obtain the virial radius,  $R_{\text{vir}}$ , for each galaxy using the formulae of Bryan & Norman (1998),

$$R_{\text{vir}}^3 = \frac{3}{4\pi} \frac{M_h}{\rho_c \Delta_c(z)} \quad \Delta_c(z) = \frac{(18\pi^2 + 82x - 39x^2)}{1+x} \quad (1)$$

where  $x = \Omega_m(1+z)^3 / [\Omega_m(1+z)^3 + \Omega_\Lambda]$ . The resulting radii have the range  $70 \leq R_{\text{vir}} \leq 840$  proper kpc with uncertainty of  $\delta R_{\text{vir}}/R_{\text{vir}} \simeq 0.1$ , where the uncertainty in each  $R_{\text{vir}}$  accounts for the standard deviation in the average virial mass assigned to each galaxy.

## 3. RESULTS

### 3.1. $W_r(2796)$ versus $D$ and $D/R_{\text{vir}}$

The observed anti-correlation between  $W_r(2796)$  and  $D$  is firmly established (e.g., Nielsen, Churchill, & Kacprzak 2012, and references therein). However, there is significant scatter in the relation. The source of the scatter has been investigated assuming a “second parameter”, i.e., galaxy luminosity (Kacprzak et al. 2008; Chen et al. 2010a), stellar mass or specific star formation rate (Chen et al. 2010b), morphology (Kacprzak et al. 2007), or geometry and orientation (Bouché et al. 2011; Kacprzak et al. 2011).

We divided the sample into halo mass quartiles. In Figure 1a, we plot  $W_r(2796)$  versus  $D$  with points col-

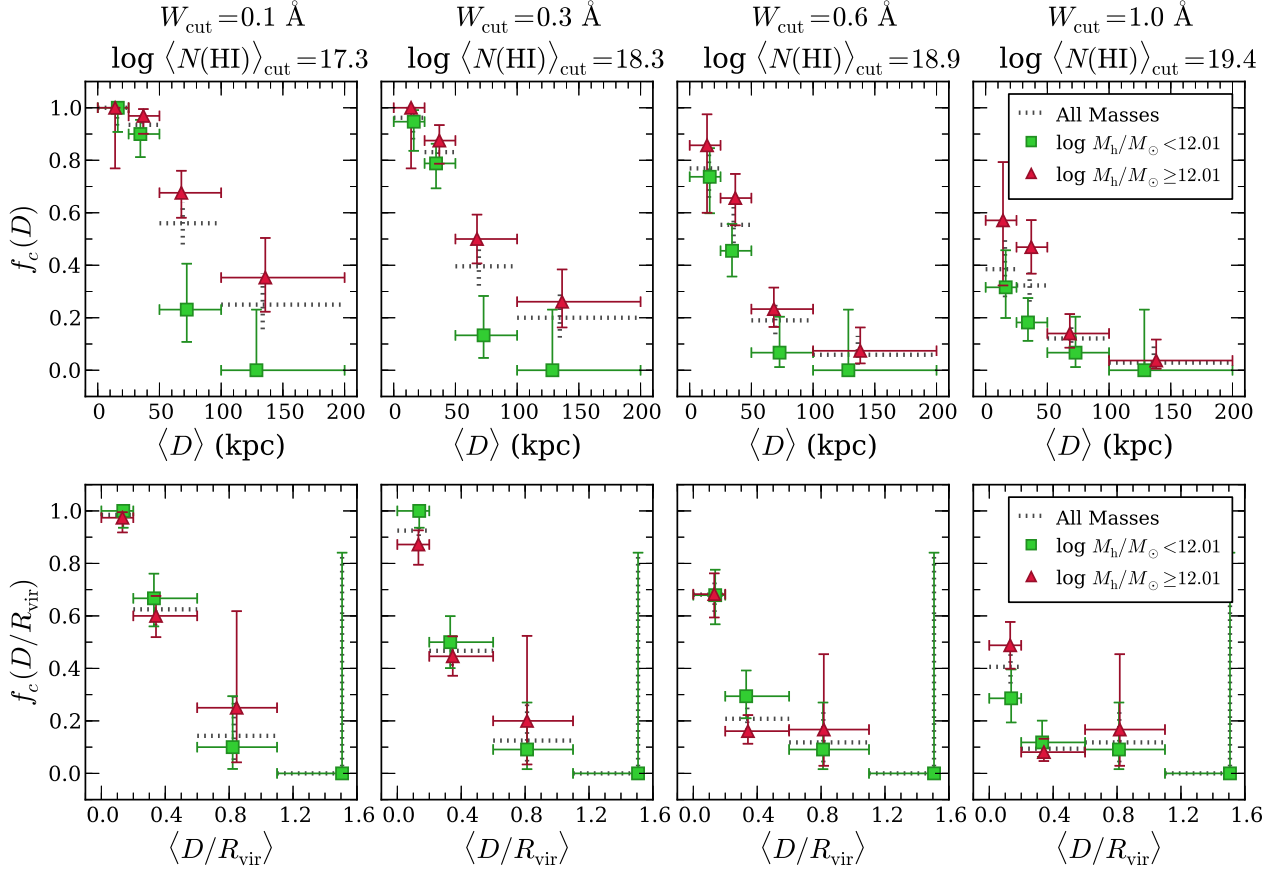


FIG. 2.— (upper panels) The CGM covering fraction,  $f_c(D)$ , for  $W_r(2796) \geq W_{\text{cut}}$  in the  $D$  bins (0,25], (25,50], (50,100], and (100,200) kpc for the high- and low-mass subsamples (dashed bars are the full sample). Each  $W_{\text{cut}}$  corresponds to a mean minimum  $\log N(\text{HI})$ . (lower panels) The covering fraction,  $f_c(D/R_{\text{vir}})$ , for  $W_r(2796) \geq W_{\text{cut}}$  in the  $D/R_{\text{vir}}$  bins (0,0.2], (0.2,0.6], (0.6,1.1], and (1.1,1.5]. High-mass halos tend to have larger  $f_c(D)$ , especially for  $D > 50$  kpc and  $W_{\text{cut}} = 0.1$  and  $0.3 \text{ \AA}$ , whereas  $f_c(D/R_{\text{vir}})$  is independent of  $M_h$ , suggesting the Mg II absorbing CGM is self-similar with halo mass.

ored by mass (see legend). The curve is a log-linear fit (Nielsen, Churchill, & Kacprzak 2012). Generally, the highest-mass halos (yellow and red points) segregate above the fitted curve, whereas the lowest-mass halos (blue and green points) segregate below the fitted curve.

In Figure 1b, we plot the data split by the median mass: the high-mass subsample (red points) has  $\log M_h/M_\odot \geq 12.01$ , and the low-mass subsample (blue points) has  $\log M_h/M_\odot < 12.01$ . A 2D Kolomorov-Smirnov (KS) test yields a  $4.2 \sigma$  significance that the null hypothesis the two subsamples have identical  $W_r(2796)$ – $D$  distributions is ruled out. Excluding galaxies with upper limits on  $W_r(2796)$  [absorbers only], the significance is  $4.0 \sigma$ . Clearly, there is significant mass segregation in the  $W_r(2796)$ – $D$  distribution, such that lower mass halos cluster toward smaller  $W_r(2796)$  and  $D$ , whereas higher mass halos cluster toward larger values.

Since halo mass is a correlated source of scatter on the  $W_r(2796)$ – $D$  plane, we examine  $W_r(2796)$  versus  $D/R_{\text{vir}}$ , since  $R_{\text{vir}} \propto (M_h)^{1/3}$ . We plot these data in Figure 1c. The solid line is the fit  $\log W_r(2796) = \alpha_1 \log(D/R_{\text{vir}}) + \alpha_2$ , using the Expectation Maximization-Likelihood method (Wolynetz 1979; Isobe, Feigelson, & Nelson 1986), which accounts for upper limits. The fit is normalized to the mean  $W_r(2796)$  of absorbing galaxies at  $D/R_{\text{vir}} = 0.3$ . We obtained  $\alpha_1 = -2.04 \pm 0.21$  and  $\alpha_2 = -1.60 \pm 0.15$ . The dashed lines are  $1 \sigma$  uncertainty curves.

A BHK- $\tau$  non-parametric rank correla-

tion test (Brown, Hollander, & Korwar 1974; Isobe, Feigelson, & Nelson 1986), which accounts for upper limits, yielded an  $8.2 \sigma$  significance for the anti-correlation between  $W_r(2796)$  and  $D$  (Nielsen, Churchill, & Kacprzak 2012). Using the BHK- $\tau$  test, we find that  $W_r(2796)$  is anti-correlated with  $D/R_{\text{vir}}$  at a  $8.9 \sigma$  significance. Relative to the fits, the variance of the data on the  $W_r(2796)$ – $D$  plane is reduced from 0.50 to 0.11 on the  $W_r(2796)$ – $D/R_{\text{vir}}$  plane (absorbers only). An  $F$ -test comparing the individual variances,  $(\log W_{\text{fit}} - \log W_i)^2$ , in both planes yielded probability  $P(F) = 1 \times 10^{-10}$  that their distributions are drawn from the same parent population; the scatter is *significantly* reduced in the  $W_r(2796)$ – $D/R_{\text{vir}}$  plane. Furthermore, the distribution of halo masses about the fit has been homogenized. A 2D KS test comparing the distributions of the low- and high-mass subsamples is consistent with their being drawn from the same parent distribution ( $1.3 \sigma$ ).

In summary, there is significant systematic mass segregation on the  $W_r(2796)$ – $D$  plane. However, on the  $W_r(2796)$ – $D/R_{\text{vir}}$  plane, the scatter about the fit is reduced with very high significance; the anti-correlation is highly significant and the segregation by mass vanishes. The data suggest that the Mg II absorbing CGM is strongly linked to halo mass such that  $W_r(2796) \propto (D/R_{\text{vir}})^{-2}$ . Interestingly, the CGM exhibits substantial “patchiness” for  $D/R_{\text{vir}} \geq 0.2$ , where the relative number of sight lines with non detections begins to increase. To investigate if this may be connected to galaxy properties,

we performed KS tests to compare the colors and luminosities of absorbing galaxies and non-absorbing galaxies with  $W_r(2796) < 0.1 \text{ \AA}$  and  $D/R_{\text{vir}} \geq 0.2$ ; we find no statistical differences.

### 3.2. Covering Fraction versus $D$ and $D/R_{\text{vir}}$

Further insight is provided by the behavior of the covering fraction of the MgII absorbing CGM, which has been investigated in some detail (Kacprzak et al. 2008; Chen et al. 2010a; Nielsen, Churchill, & Kacprzak 2012). Nielsen, Churchill, & Kacprzak (2012) showed a dependence on galaxy  $B$ -band luminosity in that higher luminosity galaxies have higher covering fractions at a given impact parameter than lower luminosity galaxies. Since luminosity is a proxy for mass, their result motivates an examination of the covering fractions as a function of  $M_h$ .

In the upper panels of Figure 2, we present  $f_c(D)$ , the CGM covering fraction in an impact parameter bin having  $W_r(2796) \geq W_{\text{cut}}$ . The uncertainties for all covering fractions presented in this work were computed using binomial statistics. We computed  $f_c(D)$  for the high-mass (red triangles) and low-mass (green squares) subsamples and for the full sample (dashed bars). Generally, high-mass halos have larger  $f_c(D)$  at  $D > 50 \text{ kpc}$  with increasing significance as  $W_{\text{cut}}$  is lowered. Note that, for  $D > 100 \text{ kpc}$ , low-mass halos have  $f_c(D) = 0$  for all  $W_{\text{cut}}$ , whereas high-mass halos have  $f_c(D) \simeq 0.3\text{--}0.1$ .

In the lower panels of Figure 2, we plot  $f_c(D/R_{\text{vir}})$ , the CGM covering fraction in a  $D/R_{\text{vir}}$  bin with  $W_r(2796) \geq W_{\text{cut}}$ . We find that  $f_c(D/R_{\text{vir}})$  for high- and low-mass halos are statistically identical;  $f_c(D/R_{\text{vir}})$  has no mass dependence for all  $W_{\text{cut}}$  at all  $D/R_{\text{vir}}$ .

Using the median fit between  $W_r(2796)$  and  $N(\text{H I})$  obtained by Ménard & Chelouche (2009), each  $W_{\text{cut}}$  converts to a mean minimum neutral hydrogen column density. However, we caution that we extrapolated below the minimum  $W_r(2796)$  of their fit ( $0.5 \text{ \AA}$ ).

The combined behavior of  $f_c(D)$  and  $f_c(D/R_{\text{vir}})$  strongly suggests that the MgII absorbing CGM is self-similar with halo mass over the range  $10.7 \leq \log M_h/M_\odot \leq 13.9$ . If so, in a fixed  $D$  bin, the higher  $f_c(D)$  values for higher mass halos is naturally explained by the fact that the CGM of higher mass halos is probed at smaller  $D/R_{\text{vir}}$ , whereas lower mass halos are probed at larger  $D/R_{\text{vir}}$ .

### 3.3. Covering Fraction versus $M_h$

In Figure 3, we present  $f_c(\leq D)$  versus  $M_h$ , where  $f_c(\leq D)$  is the CGM covering fraction within impact parameter  $D$  with  $W_r(2796) \geq W_{\text{cut}}$ . We computed  $f_c(\leq D)$  for both proper coordinates (black points) and for co-moving coordinates (open blue points). The behavior of  $f_c(\leq D)$  is not sensitive to the choice of coordinates. We find that  $f_c(\leq D)$  shows no definitive trend with  $M_h$ , being consistent with a constant value within errors.

We also computed  $f_c(\leq D/R_{\text{vir}})$ , the CGM covering fraction within  $D/R_{\text{vir}}$  with  $W_r(2796) \geq W_{\text{cut}}$ . We plot  $f_c(\leq D/R_{\text{vir}})$  versus  $M_h$  in Figure 4. Again, a suggestion of self-similarity of the MgII absorbing CGM is apparent;  $f_c(\leq D/R_{\text{vir}})$  is effectively constant with halo mass within errors, primarily depending on  $W_{\text{cut}}$  and the  $D/R_{\text{vir}}$  cut. Though a suggestion decreasing  $f_c(\leq D/R_{\text{vir}})$  with increasing  $M_h$  is visually apparent, non-parametric rank correlation tests indicate that no correlation with  $M_h$  is consistent with the data (null hypothesis satisfied within  $0.2\text{--}0.9 \sigma$ ).

Most importantly, we point out that neither  $f_c(\leq D)$  nor  $f_c(\leq D/R_{\text{vir}})$  rapidly decline or vanish for  $M_h > M_{\text{crit}}$ . This behavior is in conflict with theoretical predictions in which cold-mode accretion diminishes for  $M_h > M_{\text{crit}}$  (cf., Birnboim & Dekel 2003; Kereš et al. 2005; Dekel & Birnboim 2006; Kereš et al. 2009; Stewart et al. 2011; van de Voort et al. 2011), either implying alternative origins for a ubiquitous MgII absorbing CGM or that cold mode accretion persists above  $M_{\text{crit}}$ .

## 4. DISCUSSION AND CONCLUSIONS

We applied the halo abundance matching technique to determine the galaxy virial masses,  $M_h$ , for 183 ‘‘isolated’’ galaxies from MAGICAT (Nielsen, Churchill, & Kacprzak 2013). We report four main results:

1. To a significant degree, the substantial scatter about the  $W_r(2796)\text{--}D$  anti-correlation is explained by a systematic segregation of halo mass on the  $W_r(2796)\text{--}D$  plane. With  $4.0 \sigma$  significance, the high-mass halos exhibit larger  $W_r(2796)$  at greater  $D$  compared to the low-mass halos. The significance of the  $W_r(2796)\text{--}D/R_{\text{vir}}$  anti-correlation is  $8.9 \sigma$  and the data indicate  $W_r(2796) \propto (D/R_{\text{vir}})^{-2}$ . On the  $W_r(2796)\text{--}D/R_{\text{vir}}$  plane, systematic halo mass segregation vanishes and the scatter is reduced with very high significance. These results suggest that Mg II absorption strength is strongly linked to  $D/R_{\text{vir}}$  via halo mass.

2. For all  $W_{\text{cut}}$  and  $D/R_{\text{vir}}$ , there is no dependence of the covering fraction  $f_c(D/R_{\text{vir}})$  on  $M_h$ , whereas for smaller  $W_{\text{cut}}$  and  $D > 50 \text{ kpc}$ ,  $f_c(D)$  is higher for the high-mass halos. Since  $f_c(D/R_{\text{vir}})$  decreases with increasing  $D/R_{\text{vir}}$ , the  $M_h$  dependence of  $f_c(D)$  can be explained by the fact that at a fixed  $D$ , higher mass halos are probed at smaller  $D/R_{\text{vir}}$  and lower mass halos are probed at larger  $D/R_{\text{vir}}$ . The combined behavior of  $W_r(2796)$  versus  $D/R_{\text{vir}}$ ,  $f_c(D)$ , and  $f_c(D/R_{\text{vir}})$  strongly suggests that the MgII absorbing CGM is self-similar with halo mass over the range  $10.7 \leq \log M_h/M_\odot \leq 13.9$ .

3. The covering fraction  $f_c(\leq D)$  is constant with  $M_h$ . Similarly, the covering fraction  $f_c(\leq D/R_{\text{vir}})$  is a constant with  $M_h$  for all  $W_{\text{cut}}$  and  $D/R_{\text{vir}}$  cuts. The magnitude of the covering fraction depends only on  $W_{\text{cut}}$  and the  $D$  and  $D/R_{\text{vir}}$  cuts, decreasing with increasing  $W_{\text{cut}}$  for fixed  $D$  cut and with increasing  $D$  cut for fixed  $W_{\text{cut}}$ . The lack of dependence of  $f_c(\leq D/R_{\text{vir}})$  with  $M_h$  further supports our conclusion of the self-similarity of the Mg II absorbing CGM with halo mass.

4. Neither  $f_c(\leq D)$  nor  $f_c(\leq D/R_{\text{vir}})$  precipitously drop for  $M_h \geq M_{\text{crit}}$ . This behavior is in direct conflict with theoretical expectations of cold-mode accretion. If the MgII absorbing CGM is self-similar with halo mass, it would imply that H I in cold gas is also self-similar with halo mass.

If cold-mode accretion substantially diminishes above some  $M_{\text{crit}}$  (Birnboim & Dekel 2003; Kereš et al. 2005; Dekel & Birnboim 2006; Kereš et al. 2009; Stewart et al. 2011; van de Voort et al. 2011), our results imply that the MgII absorbing CGM must be sustained by other mechanisms in  $M_h > M_{\text{crit}}$  halos. A most obvious candidate is outflows, which are observed in starburst galaxies (e.g., Tremonti et al. 2007; Martin & Bouché 2009; Weiner et al. 2009; Rubin et al. 2010; Martin et al. 2012). On average, this would imply that, in high-mass halos, the dynamical and cooling times of non-escaping wind material are balanced with the wind cycling time scale such that their cold gas reservoirs are more-or-less observationally indistinguishable from the cold accretion reservoirs of low-mass halos. Simulations indicate recycling time scales on the order of  $0.5\text{--}1.0 \text{ Gyr}$

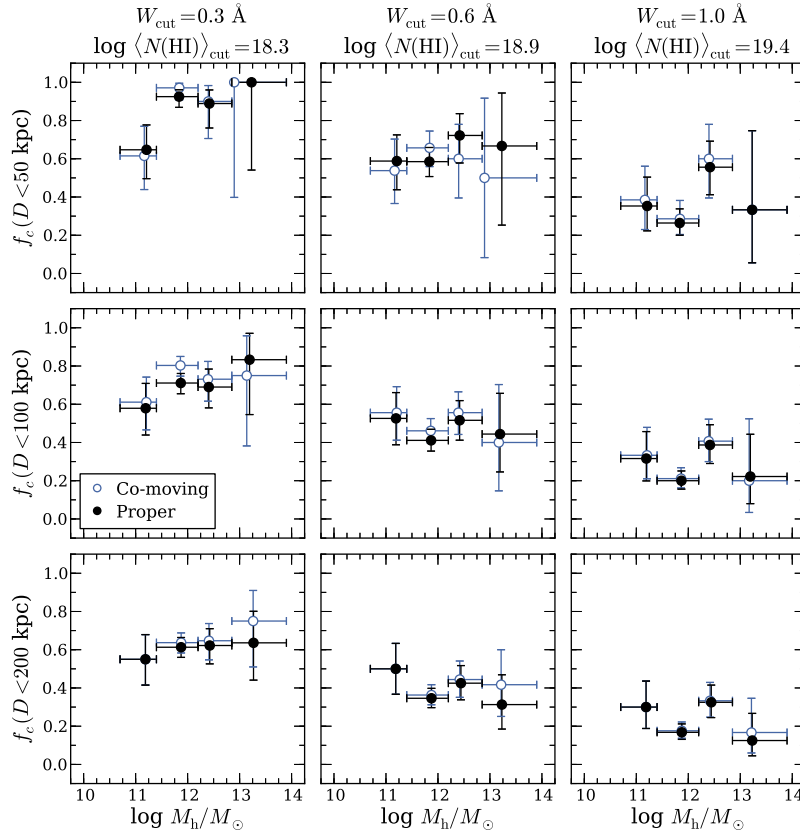


FIG. 3.— The covering fraction,  $f_c(\leq D)$  versus  $\log M_h/M_\odot$  for  $W_r(2796) \geq W_{\text{cut}}$  inside impact parameter  $D$ . Each  $W_{\text{cut}}$  corresponds to a mean minimum  $\log N(\text{HI})$ . Both proper (black points) and co-moving (open blue points) coordinates are shown. (upper)  $D \leq 50$  kpc. (middle)  $D \leq 100$  kpc. (lower)  $D \leq 200$  kpc. Contrary to theoretical expectations for cold-mode accretion, we find that  $f_c(\leq D)$  does *not* vanish for  $M_h \geq M_{\text{crit}}$ .

that decrease with increasing  $M_h$  (Oppenheimer et al. 2010; Stewart et al. 2011). Thus, galaxies in higher mass halos with quiescent star formation for longer than  $10^9$  yr would not be expected to have detectable Mg II or strong HI absorption (c.f., Churchill et al. 2012b).

On the other hand, since the number of sub-halos increases in proportion to halo mass (Klypin et al. 2011), it is plausible that absorption from sub-halos counteracts our ability to observe the cut off of cold-mode accretion in the central halos with  $M_h \geq M_{\text{crit}}$ . Alternatively, the theoretical prediction that cold-mode accretion universally diminishes in higher mass halos may not be correct.

Since  $R_{\text{vir}} \propto (M_h/\Delta_c)^{1/3}$  and  $W_r(2796) \propto (D/R_{\text{vir}})^{-2}$ , we deduce that  $W_r(2796) \propto D^{-2}(M_h/\Delta_c)^{2/3}$  over the range  $10.7 \leq M_h \leq 13.9$ . That is,  $W_r(2796) \propto D^{-2}$  for fixed  $M_h$  and  $W_r(2796) \propto (M_h/\Delta_c)^{2/3}$  for fixed  $D$ . This behavior is consistent with the halo mass segregation we observe on the  $W_r(2796)$ – $D$  plane, and is corroborated by the  $W_r(2796)$ –stellar mass correlation reported by Martin et al. (2012)

for starburst galaxies and the stellar mass dependence on the halo cross section of Mg II absorbing gas (Chen et al. 2010b). However, it is contrary to the global  $W_r(2796)$ – $M_h$  anti-correlation reported by Bouché et al. (2006) and Gauthier et al. (2009) based upon cross-correlation techniques. We explore implications of this discrepancy in Churchill et al. (2013).

We thank Peter Behroozi for insightful discussions during his visit to NMSU and Jean-René Gauthier for valuable input. CWC and NMN were partially supported through grant HST-GO-12252 provided by NASA’s Space Telescope Science Institute, which is operated by AURA under NASA contract NAS 5-26555. NMN was also partially supported through a NMSGC Graduate Fellowship and a three-year Graduate Research Enhancement Grant (REG) sponsored by the Office of the Vice President for Research at New Mexico State University. Dedicated to the memory of William Arthur Churchill.

#### REFERENCES

- Behroozi, P. S., Conroy, C., & Wechsler, R. H. 2010, *ApJ*, 717, 379  
 Bouché, N., Murphy, M. T., Péroux, C., Csabai, I., & Wild, V. 2006, *MNRAS*, 371, 495  
 Bouché, N., Hohensee, W., Vargas, R., et al. 2011, *MNRAS*, 426, 801  
 Birnboim, Y., & Dekel, A. 2003, *MNRAS*, 345, 349  
 Bolzonella, M., Miralles, J.-M., & Pelló, R. 2000, *A&A*, 363, 476  
 Brown, B. W., Hollander, M., & Korwar, R. M. 1974, in *Reliability and Biometry*, 327  
 Bryan, G. L., & Norman, M. L. 1998, *ApJ*, 495, 80  
 Chen, H.-W., Helsby, J. E., Gauthier, J.-R., Shectman, S. A., Thompson, I. B., & Tinker, J. L. 2010a, *ApJ*, 714, 1521  
 Chen, H.-W., Wild, V., Tinker, J. L., et al. 2010b, *ApJ*, 724, L176  
 Churchill, C. W., Kacprzak, G. G., Nielsen, N. M., Steidel, C. C., & Murphy, M. T. 2012a, *ApJ*, submitted  
 Churchill, C. W., Kacprzak, G. G., & Steidel, C. C. 2005, in *Probing Galaxies through Quasar Absorption Lines*, IAU 199 Proceedings, eds. P. R. Williams, C.-G. Shu, & B. Ménard (Cambridge: Cambridge University Press), p. 24

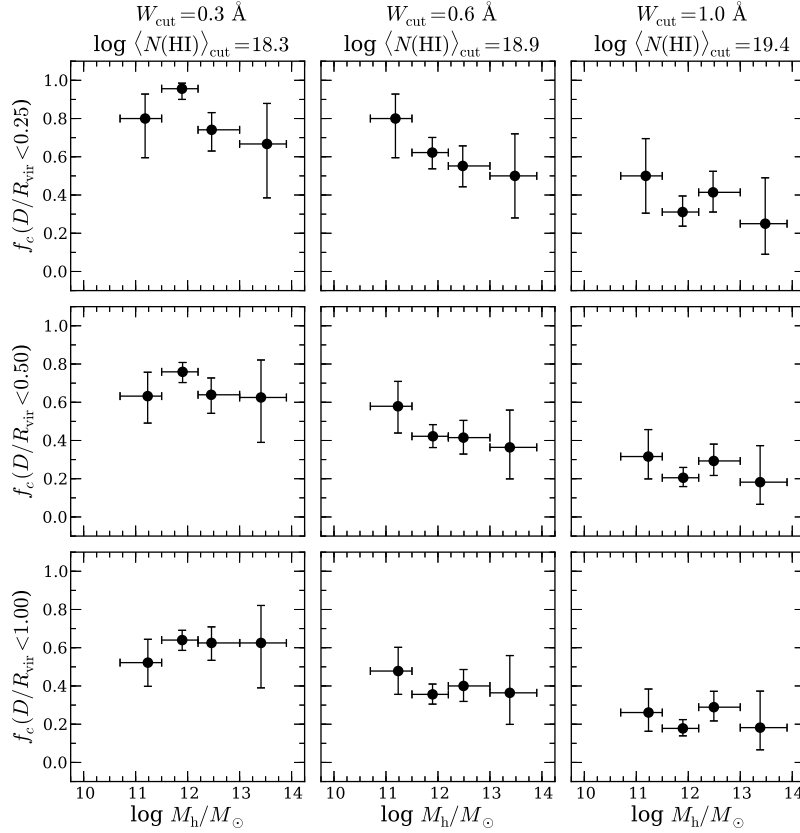


FIG. 4.— The CGM covering fraction,  $f_c(\leq D/R_{\text{vir}})$ , versus  $\log M_h/M_\odot$  for  $W_r(2796) \geq W_{\text{cut}}$  inside fractional projection  $D/R_{\text{vir}}$ . Each  $W_{\text{cut}}$  corresponds to a mean minimum  $\log N(\text{HI})$ . (top)  $D/R_{\text{vir}} \leq 0.25$ . (middle)  $D/R_{\text{vir}} \leq 0.5$ . (bottom)  $D/R_{\text{vir}} \leq 1.0$ . Though the data hint that  $f_c(\leq D/R_{\text{vir}})$  may decrease with increasing  $\log M_h$ , the trends are not statistically significant for our sample. The data suggest self-similarity of the covering fraction with halo mass, with  $f_c(\leq D/R_{\text{vir}})$  depending primarily on  $W_{\text{cut}}$  and the  $D/R_{\text{vir}}$  cut.

Churchill, C. W., Kacprzak, G. G., Steidel, C. C., et al. 2012b, arXiv: 1205.0595  
Churchill, C. W., Nielsen, N. M., Kacprzak, G. G., & Trujillo-Gomes, S. 2013, ApJ, in preparation  
Churchill, C. W., Mellon, R. R., Charlton, J. C., Jannuzi, B. T., Kirhakos, S., Steidel, C. C., & Schneider, D. P. 2000, ApJS, 130, 91  
Churchill, C. W., Rigby, J. R., Charlton, J. C., & Vogt, S. S. 1999, ApJS, 120, 51  
Coleman, G. D., Wu, C.-C., & Weedman, D. W. 1980, ApJS, 43, 393  
Conroy, C., Wechsler, R. H., & Kravtsov, A. V. 2006, ApJ, 647, 201  
Conroy, C., & Wechsler, R. H. 2009, ApJ, 696, 620  
Dekel, A., & Birnboim, Y. 2006, MNRAS, 368, 2  
Gauthier, J.-R., Chen, H.-W., & Tinker, J. L. 2009, ApJ, 702, 50  
Isobe, T., Feigelson, E. D., & Nelson, P. I. 1986, ApJ, 306, 490  
Kacprzak, G. G., Churchill, C. W., Steidel, C. C., & Murphy, M. T. 2008, AJ, 135, 922  
Kacprzak, G. G., Churchill, C. W., Evans, J. L., Murphy, M. T., & Steidel, C. C. 2011, MNRAS, 416, 3118  
Kacprzak, G. G., Churchill, C. W., Steidel, C. C., Murphy, M. T., & Evans, J. L. 2007, ApJ, 662, 909  
Kacprzak, G. G., Churchill, C. W., Steidel, C. C., Spitler, L. R., Holtzman, J. A., & Bouché, N. A. 2012, MNRAS, in press (arXiv:1208.4098)  
Kereš, D., Katz, N., Fardal, M., Davé, R., & Weinberg, D. H. 2009, MNRAS, 395, 160  
Kereš, D., Katz, N., Weinberg, D. H., & Davé, R. 2005, MNRAS, 363, 2  
Kim, A., Goobar, A., & Perlmutter, S. 1996, PASP, 108, 190

Klypin, A. A., Trujillo-Gomez, S., & Primack, J. 2011, ApJ, 740, 102  
Martin, C. L., & Bouché, N. 2009, ApJ, 703, 1394  
Martin, C. L., Shapley, A. E., Coil, A. L., et al. 2012, arXiv:1206.5552  
Ménard, B., & Chelouche, D. 2009, MNRAS, 393, 808  
Nielsen, N. M., Churchill, C. W., & Kacprzak, G. G. 2012, ApJ, submitted (arXiv:1211.1380)  
Nielsen, N. M., Churchill, C. W., & Kacprzak, G. G. 2013, ApJ, in prep  
Oppenheimer, B. D., Davé, R., Kereš, D., et al. 2010, MNRAS, 406, 2325  
Rao, S. M., & Turnshek, D. A. 2000, ApJS, 130, 1  
Ribaldo, J., Lehner, N., Howk, J. C., et al. 2011, ApJ, 743, 207  
Rigby, J. R., Charlton, J. C., & Churchill, C. W. 2002, ApJ, 565, 743  
Rodriguez-Puebla, A., Drory, N., & Avila-Reese, V. 2012, arXiv:1204.0804  
Rubin, K. H. R., Weiner, B. J., Koo, D. C., et al. 2010, ApJ, 719, 1503  
Stewart, K. R., Kaufmann, T., Bullock, J. S., et al. 2011, ApJ, 735, L1  
Trujillo-Gomez, S., Klypin, A., Primack, J., & Romanowsky, A. J. 2011, ApJ, 742, 16  
Thom, C., Werk, J. K., Tumlinson, J., et al. 2011, ApJ, 736, 1  
Tremonti, C. A., Moustakas, J., & Diamond-Stanic, A. M. 2007, ApJL, 663, L77  
Tumlinson, J., Thom, C., Werk, J. K., et al. 2011, Science, 334, 948  
van de Voort, F., Schaye, J., Booth, C. M., Haas, M. R., & Dalla Vecchia, C. 2011, MNRAS, 414, 2458  
Wang, W., & Wells, M. T. 2000,  
Weiner, B. J., et al. 2009, ApJ, 692, 187  
Wolf, C., Meisenheimer, K., Rix, H.-W., et al. 2003, A&A, 401, 73  
Wolynetz, M. S. 1979, Journal of the Royal Statistical Society, 28, 195